Syntheses, Structures, and Physical Properties of LnAsTe (Ln = La, Pr, Sm, Gd, Dy, Er)

Fu Qiang Huang,[†] Paul Brazis,[‡] Carl R. Kannewurf,[‡] and James A. Ibers*,[†]

Department of Chemistry and Department of Electrical and Computer Engineering, Northwestern University, 2145 Sheridan Road, Evanston, Illinois 60208

Received February 22, 2000

Six rare-earth arsenic tellurides have been synthesized by the reactions of the rare-earth elements (Ln) with As and Te at 1123 K. LaAsTe (a = 7.8354(11) Å, b = 4.1721(6) Å, c = 10.2985(14) Å, T = 153 K), PrAsTe (a = 7.728(2) Å, b = 4.1200(11) Å, c = 10.137(3) Å, T = 153 K), SmAsTe (a = 7.6180(16) Å, b = 4.0821(9) Å, c = 9.991(2) Å, T = 153 K), GdAsTe (a = 7.5611(15) Å, b = 4.0510(8) Å, c = 9.920(2) Å, T = 153 K), DyAsTe (a = 7.4951(13) Å, b = 4.0246(7) Å, c = 9.8288(17) Å, T = 153 K), and ErAsTe (a = 7.4478(1) Å, b = 4.0078(1) Å, c = 9.7552(2) Å, T = 153 K) crystallize with four formula units in the orthorhombic space group D_{2h}^{16}-*Pnma*. These compounds are isostructural and belong to the β-$ZrSb_2$ structure type. In each compound, the Ln atoms are coordinated by a tricapped trigonal prism of four As atoms and five Te atoms. The entire three-dimensional structure is built up by the motif of the $LnAs_4Te_5$ tricapped trigonal prisms. Infinite nonalternating zigzag As chains are found along the b axis, with As−As distances in these compounds ranging from 2.5915(5) to 2.6350(9) Å. Conductivity measurements in the direction of these As chains indicate that PrAsTe is metallic whereas SmAsTe and DyAsTe are weakly metallic. Antiferromagnetic transitions occur in SmAsTe and DyAsTe at 3 and 9 K, respectively. DyAsTe above 9 K follows the Curie−Weiss law.

Introduction

The study of low-dimensional solids is an important aspect of solid-state chemistry.[1,2] Such solids can exhibit interesting physical properties, including superconductivity and charge density waves.[3−5] One subgroup of low-dimensional solids comprises compounds in which there are one-dimensional chains of closely spaced atoms. Such systems display a variety of specific physical phenomena. These very simple systems are especially interesting because chemical correlations between structure and properties are more easily arrived at than in more complex topologies.[6] A number of structure types are known that contain infinite zigzag chains of groups IIIA−VA elements. These include the structure types CrB,[7−10] FeB,[7,8,11] MoB,[7,12,13] $ZrSi_2$,[7,14−16] $CeNiSi_2$,[7,17,18] $SmNiGe_3$,[19] β-$ZrSb_2$,[20,21] $HoSb_2$,[22,23] $CaSb_2$,[7,24−26] and CeAsS.[27−29]

Consider now infinite zigzag chains of group VA atoms. In some of these chains the atoms are equidistant. For example, in β-$ZrSb_2$ each Sb atom in the zigzag Sb chain has two Sb neighbors at a distance of 2.890(1) Å.[20] But in others, the chains are distorted. For example, in the $CaSb_2$ structure, each Sb atom has Sb neighbors at 2.915(1) and 2.939(1) Å.[24] Distorted zigzag As chains are found in the CeAsS family, which includes the LnAsS and LnAsSe phases (Ln = rare-earth element).[27−29] Distorted zigzag P chains are found in the structures of PdP_2[30]

[†] Department of Chemistry.
[‡] Department of Electrical and Computer Engineering.

(1) Rouxel, J., Ed. *Crystal Chemistry and Properties of Materials with Quasi-one-dimensional Structures*; Physics and Chemistry of Materials with Low-Dimensional Structures. Series B, Quasi-One-Dimensional Materials; D. Reidel: Dordrecht, The Netherlands, 1986.
(2) Monceau, P., Ed. *Electronic Properties of Inorganic Quasi-one-dimensional Compounds*; Physics and Chemistry of Materials with Low-dimensional Structures. Series B, Quasi-One-Dimensional Materials; D. Reidel: Dordrecht, The Netherlands, 1985; Parts I and II.
(3) Withers, R. L.; Wilson, J. A. *J. Phys. C: Solid State Phys.* **1986**, *19*, 4809−4845.
(4) Chaussy, J.; Haen, P.; Lasjaunias, J. C.; Monceau, P.; Waysand, G.; Waintal, A.; Meerschaut, A.; Molinié, P.; Rouxel, J. *Solid State Commun.* **1976**, *20*, 759−763.
(5) Monceau, P.; Ong, N. P.; Portis, A. M.; Meerschaut, A.; Rouxel, J. *Phys. Rev. Lett.* **1976**, *37*, 602−606.
(6) Day, P. In *Solid State Chemistry Compounds*; Cheetham, A. K., Day, P., Eds.; Clarendon Press: Oxford, 1992; pp 31−59.
(7) Villars, P., Calvert, L. D., Eds. *Pearson's Handbook of Crystallographic Data for Intermetallic Phases*, 2nd ed.; ASM International: Materials Park, OH, 1991; Vol. 1.
(8) Hohnke, D.; Parthé, E. *Acta Crystallogr.* **1966**, *20*, 572−582.
(9) Frueh, A. J., Jr. *Acta Crystallogr.* **1951**, *4*, 66−67.
(10) Rieger, W.; Parthé, E. *Acta Crystallogr.* **1967**, *22*, 919−922.
(11) Decker, B. F.; Kasper, J. S. *Acta Crystallogr.* **1954**, *7*, 77−80.
(12) Kiessling, R. *Acta Chem. Scand.* **1947**, *1*, 893−916.
(13) Haschke, H.; Nowotny, H.; Benesovsky, F. *Monatsh. Chem.* **1966**, *5*, 1459−1568.
(14) Náray-Szabó, St. v. *Z. Kristallogr., Kristallgeom., Kristallphys., Kristallchem.* **1937**, *97*, 223−228.
(15) Schachner, H.; Nowotny, H.; Kudielka, H. *Monatsh. Chem.* **1964**, *85*, 1141−1153.
(16) Wang, R.; Bodnar, R.; Steinfink, H. *Inorg. Chem.* **1966**, *8*, 1468−1470.
(17) Proserpio, D. M.; Chacon, G.; Zheng, C. *Chem. Mater.* **1998**, *10*, 1286−1290.
(18) Gladyshevskii, R. E.; Cenzual, K.; Zhao, J. T.; Parthé, E. *Acta Crystallogr., Sect. C: Cryst. Struct. Commun.* **1992**, *48*, 221−225.
(19) Chen, X. Z.; Larson, P.; Sportouch, S.; Brazis, P.; Mahanti, S. D.; Kannewurf, C. R.; Kanatzidis, M. G. *Chem. Mater.* **1999**, *11*, 75−83.
(20) Garcia, E.; Corbett, J. D. *J. Solid State Chem.* **1988**, *73*, 452−467.
(21) Lam, R.; Mar, A. *J. Solid State Chem.* **1997**, *134*, 388−394.
(22) Johnson, Q. *Inorg. Chem.* **1971**, *10*, 2089−2090.
(23) Eatough, N. L.; Hall, H. T. *Inorg. Chem.* **1969**, *8*, 1439−1445.
(24) Deller, K.; Eisenmann, B. *Z. Anorg. Allg. Chem.* **1976**, *425*, 104−108.
(25) Deller, K.; Eisenmann, B. *Z. Naturforsch., B: Anorg. Chem., Org. Chem.* **1976**, *31*, 1146−1147.
(26) Hulliger, F.; Schmelczer, R. *J. Solid State Chem.* **1978**, *26*, 389−396.
(27) Céolin, R.; Khodadad, P.; Sfez, G. *C. R. Acad. Sci. Paris* **1972**, *274*, 1731−1734.
(28) Schmelczer, R.; Schwarzenbach, D.; Hulliger, F. *Z. Naturforsch., B: Anorg. Chem., Org. Chem.* **1981**, *36*, 463−469.
(29) Céolin, R.; Rodier, N.; Khodadad, P. *J. Less-Common Met.* **1977**, *53*, 137−140.

10.1021/ic000187v CCC: $19.00
Published on Web 06/22/2000

Table 1. Crystal Data and Structure Refinement for LaAsTe, PrAsTe, SmAsTe, GdAsTe, DyAsTe, and ErAsTe[a]

compd	LaAsTe	PrAsTe	SmAsTe	GdAsTe	DyAsTe	ErAsTe
fw	341.43	343.43	352.87	359.77	365.02	369.78
a (Å)	7.8354(11)	7.728(2)	7.6180(16)	7.5611(15)	7.4951(13)	7.4478(1)
b (Å)	4.1721(6)	4.1200(11)	4.0821(9)	4.0510(8)	4.0246(7)	4.0078(1)
c (Å)	10.2985(14)	10.137(3)	9.991(2)	9.920(2)	9.8288(17)	9.7552(2)
V (Å^3)	336.66(8)	322.74(15)	310.71(11)	303.84(10)	296.48(9)	291.186(10)
d_{calcd} (g/cm^3)	6.736	7.068	7.598	7.865	8.178	8.435
linear abs coeff (cm^{-1})	306.30	338.11	386.13	417.06	455.74	495.63
$R(F)^b$ ($F_o^2 > 2\sigma(F_o^2)$)	0.0261	0.0246	0.0270	0.0354	0.0237	0.0279
$R_w(F_o^2)^c$ (all data)	0.0862	0.0599	0.0670	0.0819	0.0620	0.0706

[a] For all compounds: space group D_{2h}^{16}-*Pnma*, $Z = 4$, $T = 153(2)$ K, and λ (Mo Kα) = 0.710 73 Å. [b] $R(F) = \sum||F_o| - |F_c||/\sum|F_o|$. [c] $R_w(F_o^2) = [\sum w(F_o^2 - F_c^2)^2/\sum wF_o^4]^{1/2}$, $w^{-1} = \sigma^2(F_o^2) + (0.04F_o^2)^2$ for $F_o^2 \geq 0$; $w^{-1} = \sigma^2(F_o^2)$ for $F_o^2 < 0$.

Table 2. Selected Bond Lengths (Å) and Angles (deg) in the Structures of LaAsTe, PrAsTe, SmAsTe, GdAsTe, DyAsTe, and ErAsTe

compound[a]	LaAsTe	PrAsTe	SmAsTe	GdAsTe	DyAsTe	ErAsTe
Ln−As (1)	3.1235(9)	3.0780(10)	3.0351(9)	3.0143(9)	2.9885(8)	2.9668(4)
Ln−As × 2 (2)	3.2493(7)	3.1951(7)	3.1474(7)	3.1198(6)	3.0889(6)	3.0671(3)
Ln−As (3)	3.3100(9)	3.2474(10)	3.1924(9)	3.1620(9)	3.1282(8)	3.1033(4)
Ln−Te × 2 (1)	3.2256(5)	3.1805(6)	3.1406(6)	3.1173(5)	3.0920(5)	3.0731(2)
Ln−Te × 2 (2)	3.2360(6)	3.1900(7)	3.1506(6)	3.1291(6)	3.1043(6)	3.0873(2)
Ln−Te (3)	3.3151(7)	3.2816(9)	3.2494(8)	3.2301(8)	3.2088(7)	3.1922(3)
As−As × 2	2.6350(9)	2.6206(9)	2.6098(9)	2.6035(9)	2.5982(8)	2.5915(5)
As−As−As	104.68(5)	103.64(4)	102.90(5)	102.15(5)	101.52(4)	101.29(3)

[a] The numbers in parentheses correspond to those in Figure 4.

and LaP_2,[31] whereas in the GdPS family, which includes the LnPS phases,[32,33] distorted cis−trans chains of P atoms are found. The formation of such chains is considered to be caused by the distortion of a square net.[34,35]

The present study is concerned with the Ln−As−Te system. There appear to be no known examples of this system except for Eu_4As_2Te, which has the anti-Th_3P_4 structure type.[36] Here, we present the syntheses, structures, and physical properties of LnAsTe (Ln = La, Pr, Sm, Gd, Dy, Er). These compounds, which belong to the β-$ZrSb_2$[20,21] (or $PbCl_2$) structure type, contain undistorted zigzag As chains.

Experimental Details

Syntheses. The compounds LnAsTe (Ln = La, Pr, Sm, Gd, Dy, Er) were prepared by the reactions of the rare-earth elements La (Reacton, 99.9%), Pr (Alfa, 99.9%), Sm (Alfa, 99.9%), Gd (Alfa, 99.9%), Dy (Aldrich, 99.9%), and Er (Alfa, 99.9%) with As (Alfa, 99.999%) and Te (Aldrich, 99.8%) in a KCl/LiCl flux (55:45 molar ratio). Mixtures of 1.0 mmol of Ln, 1.0 mmol of As, 1.0 mmol of Te, and 500 mg of KCl/LiCl were loaded into fused-silica tubes under an argon atmosphere in a glovebox. These tubes were sealed under 10^{-4} Torr and then placed in a computer-controlled furnace. The samples were heated to 1123 K at 1 K/min, kept at 1123 K for 3 days, slowly cooled at 0.05 K/min to 573 K, then cooled to room temperature. The reaction mixtures were washed free of chloride salts with water and then dried with acetone. In each reaction the major component consisted of black needles. Analysis of these needles with an energy dispersive X-ray (EDX)-equipped Hitachi S-4500 scanning electron microscope showed only the presence of Ln, As, and Te in the approximate ratio of 1:1:1. These compounds are stable in air.

Structure Determinations. Single-crystal X-ray diffraction data were collected with the use of graphite-monochromatized Mo Kα radiation (λ = 0.710 73 Å) at 153 K on a Bruker Smart-1000 CCD diffractometer with the program SMART.[37] The crystal-to-detector distance was 5.023 cm. Crystal decay was monitored by re-collecting 50 initial frames at the end of data collection. Data were collected by a scan of 0.3° in ω in groups of 606 frames at φ settings of 0°, 120°, and 240°. The exposure times were 20 s/frame for LaAsTe, SmAsTe, GdAsTe, and ErAsTe, 15 s/frame for PrAsTe, and 25 s/frame for DyAsTe. Cell refinement and data reduction were carried out with the use of the program SAINT,[37] and face-indexed absorption corrections were performed numerically with the use of XPREP.[38] Then the program SADABS[37] was employed to make incident beam and decay corrections.

All the structures were solved by means of the direct methods program SHELXS of the SHELXT.PC suite of programs[38] and were refined by full-matrix least-squares techniques.[38] The final refinements included anisotropic displacement parameters and secondary extinction corrections. These displacement parameters do not suggest the presence of significant nonstoichiometry. Additional experimental details are shown in Table 1 and in Supporting Information. Table 2 presents selected bond distances and angles.

Electrical Conductivity. Conductivity measurements were made along the b axis (the direction of the infinite zigzag As chains) as a function of temperature for PrAsTe, SmAsTe, and DyAsTe. For each of these compounds the composition of two single crystals was confirmed with EDX measurements. The electrical conductivity of each single crystal was measured with the use of a computer-controlled, four-probe technique.[39] Electrical contacts consisted of fine gold wire (25 and 60 μm in diameter) attached to the crystals with gold paste. Samples were placed under vacuum for at least 24 h to allow the gold paste to dry completely, which improved contact performance. Excitation currents were kept as low as possible, typically below 1 mA, to minimize any nonohmic voltage response and thermoelectric effects at the contact−sample interface. Measurements of the sample cross-sectional area and voltage probe separation were made with a calibrated binocular microscope.

Thermopower Measurements. Variable-temperature thermopower data were taken with the use of a slow-ac measurement technique.[40]

(30) Zachariasen, W. H. *Acta Crystallogr.* **1963**, *16*, 1253−1255.
(31) von Schnering, H. G.; Wichelhaus, W.; Nahrup, M. S. *Z. Anorg. Allg. Chem.* **1975**, *412*, 193−201.
(32) Hulliger, F. *Nature (London)* **1968**, *219*, 373−374.
(33) Hulliger, F.; Schmelczer, R.; Schwarzenbach, D. *J. Solid State Chem.* **1977**, *21*, 371−374.
(34) Keszler, D. A.; Hoffmann, R. *J. Am. Chem. Soc.* **1987**, *109*, 118−124.
(35) Tremel, W.; Hoffmann, R. *J. Am. Chem. Soc.* **1987**, *109*, 124−140.
(36) Hulliger, F. *Mater. Res. Bull.* **1979**, *14*, 259−262.
(37) *SMART Version 5.054 Data Collection and SAINT-Plus Version 6.0 Data Processing Software for the SMART System*; Bruker Analytical X-Ray Instruments, Inc.: Madison, WI, 1999.
(38) Sheldrick, G. M. *SHELXTL DOS/Windows/NT*, version 5.10; Bruker Analytical X-Ray Instruments, Inc.: Madison, WI, 1997.
(39) Lyding, J. W.; Marcy, H. O.; Marks, T. J.; Kannewurf, C. R. *IEEE Trans. 1nstrum. Meas.* **1988**, *37*, 76−80.

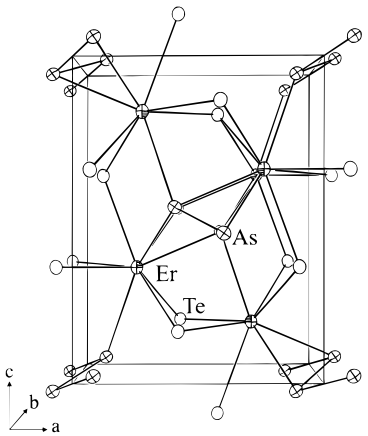

Figure 1. Unit cell of ErAsTe. The 90% displacement ellipsoids are displayed.

Table 3. Atomic Parameters Used for the Extended Hückel Calculations

element	orbital	H_{ii} (eV)	ζ_1	ζ_1	C_1	C_2
La	6s	−7.67	2.14			
	6p	−5.01	2.08			
	5d	−8.21	3.78	1.381	0.7765	0.4586
As	4s	−16.22	2.23			
	4p	−12.16	1.89			
Te	5s	−21.20	2.51			
	5p	−12.50	2.16			

The measurement apparatus featured Au(0.07% Fe)/Chromel differential thermocouples for monitoring the applied temperature gradients. Samples were mounted on 60 μm gold wire by means of gold paste. Fine gold wire (10 μm in diameter) was used for sample voltage contacts, which were made as long as possible in order to minimize thermal conduction through the leads. The sample and thermocouple voltages were measured with the use of Keithley model 181 and Keithley model 182 nanovoltmeters, respectively. The applied temperature gradient was in the range 0.1−0.4 K. Measurements were taken under a turbopumped vacuum maintained below 10^{-5} Torr. The sample chamber was evacuated for 1−3 h prior to cooling to remove any residual water vapor or solvents in the gold paste.

Magnetic Susceptibility. An 18 mg sample of SmAsTe and a 27 mg sample of DyAsTe containing single crystals were used for magnetic susceptibility measurements over the temperature range 2−300 K. The composition of each sample was verified by EDX measurements. The magnetization was measured at 200 and 100 G for SmAsTe and DyAsTe, respectively, between 5 and 300 K with the use of a Quantum Design superconducting quantum interference device (SQUID) magnetometer. All measurements were corrected for core diamagnetism.[41]

Extended Hückel Calculations. All calculations were performed on LaAsTe with the use of the YAeHMOP package.[42−44] The atomic parameters are listed in Table 3. Band structure calculations were carried out for a zigzag As chain and for the entire LaAsTe structure.

Results and Discussion

The compounds LnAsTe (Ln = La, Pr, Sm, Gd, Dy, Er) are isostructural; the unit cell of ErAsTe is displayed in Figure 1. LnAsTe adopts the β-$ZrSb_2$ structure,[20] which is of the $PbCl_2$ type. The three crystallographically independent atoms—Zr, Sb1, Sb2—in β-$ZrSb_2$ are replaced by Ln, As, and Te, respectively, in LnAsTe. In each of the present structures the Ln atom is coordinated by five Te atoms and four As atoms at the vertices of a tricapped trigonal prism in which two As atoms and one Te atom constitute the cap (Figure 1 and Figure 2a). This $LnAs_4Te_5$ tricapped trigonal prism is the motif from which the three-dimensional structure of LnAsTe is constructed. In this prism three of the four As atoms are bonded neighbors (Figure 2a). These prisms are joined in such a way to result in a one-dimensional zigzag chain of As atoms along the *b* direction (Figure 3a). Note that the tricapped trigonal prisms UPn_4Q_5 and $LnPn_4Q_5$ are also the motifs in the structures of UPnQ,[45] LaSbTe,[46] and LnPnQ (Pn = P, As; Q = S, Se).[27,29,32,33] In the structures of UPnQ and LaSbTe, four Pn atoms in the tricapped trigonal prism form a Pn square net. In the structures of LnPnQ, four Pn atoms are also neighbors and lie in a plane, but they form zigzag As chains in LnAsQ or cis−trans P chains in LnPQ. Although LnAsTe and LnAsQ (Q = S, Se) both comprise infinite zigzag As chains, their structures are completely different because the motifs from which they are constructed are different (Figure 2). Figure 3 displays structural fragments of LnAsTe and LnAsQ (Q = S, Se). All the zigzag As chains in LnAsQ (Q = S, Se) are parallel to each other, but the zigzag As chains in LnAsTe are not.

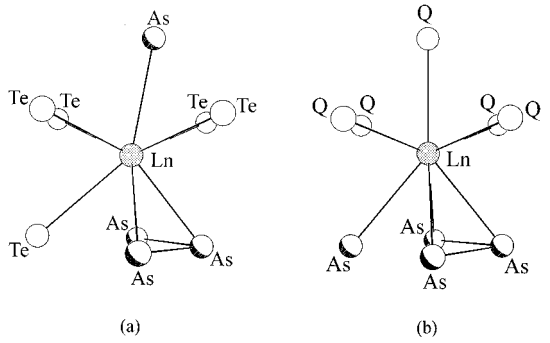

Figure 2. (a) $LnAs_4Te_5$ polyhedral motif of LnAsTe. (b) $LnAs_4Se_5$ polyhedral motif of LnAsQ (Q = S, Se).

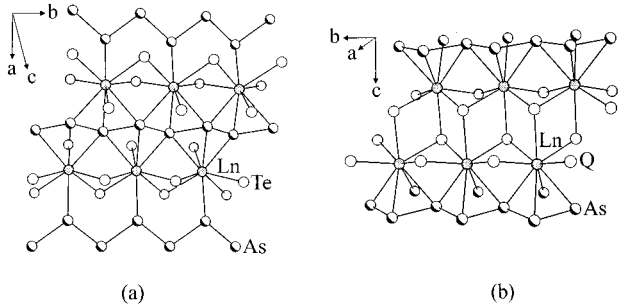

Figure 3. Part of the structures of (a) LnAsTe and (b) LnAsQ (Q = S, Se).

The Ln−Te, Ln−As, and As−As distances in LnAsTe are normal. To take GdAsTe as an example, the Gd−Te distances that range from 3.1173(5) to 3.2301(8) Å are comparable with Gd−Te distances in Gd_2Te_3 of 3.104(1) to 3.683(1) Å;[47] the Gd−As distances of 3.0143(9) to 3.1620(9) Å are close to those in GdAsSe of 3.088(2) to 3.164(2) Å;[28] the As−As distance of the zigzag As chain of 2.6035(9) Å may be compared with the

(40) Marcy, H. O.; Marks, T. J.; Kannewurf, C. R. *IEEE Trans. Instrum. Meas.* **1990**, *39*, 756−760.
(41) Mulay, L. N., Boudreaux, E. A., Eds. *Theory and Applications of Molecular Diamagnetism*; Wiley-Interscience: New York, 1976.
(42) Landrum, G. *Yet Another Extended Hückel Molecular Orbital Package (YAeHMOP)*, version 2.0; 1997. This program is available free of charge at http://overlap.chem.cornell.edu:8080/yaehmop.html.
(43) Hoffmann, R. *J. Chem. Phys.* **1963**, *39*, 1397−1412.
(44) Whangbo, M.-H.; Hoffmann, R. *J. Am. Chem. Soc.* **1978**, *100*, 6093−6098.
(45) Haneveld, A. J. K.; Jellinek, F. *J. Less-Common Met.* **1969**, *18*, 123−129.
(46) Wang, R.; Steinfink, H.; Raman, A. *Inorg. Chem.* **1967**, *6*, 1298−1300.
(47) Swinnea, J. S.; Steinfink, H.; Danielson, L. R. *J. Appl. Crystallogr.* **1987**, *20*, 102−104.

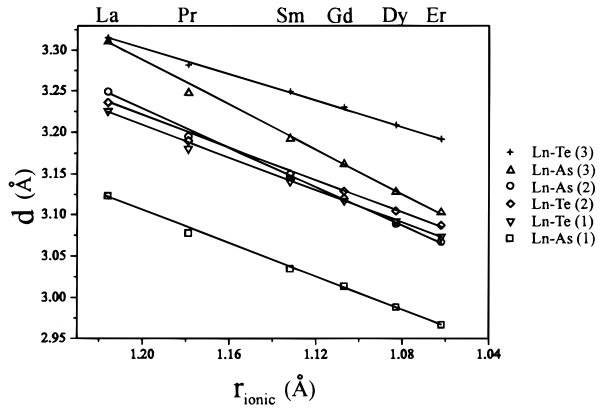

Figure 4. Plots of the Ln−As and Ln−Te distances vs ionic radii[52] of nine-coordinated Ln^{3+}.

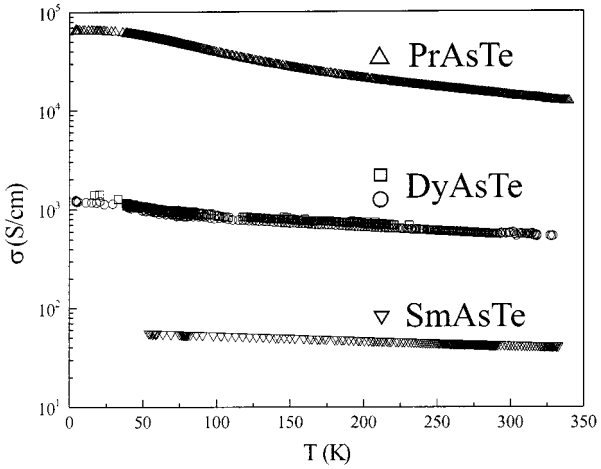

Figure 5. Semilog plot of conductivity (σ) vs temperature (T) for PrAsTe, SmAsTe, and DyAsTe.

distances of 2.656(3) and 2.662(3) Å in GdAsSe[28] and the As−As single bond distance in elemental As of 2.516(1) Å.[48] As shown in Table 2, the As−As distance in the chain decreases from 2.6350(9) to 2.5915(5) Å across the series from La to Er, and the As−As−As angle decreases from 104.68(5)° to 101.29(3)°. Other bond lengths involving Ln in Table 2 decrease almost linearly across the series from La to Er (Figure 4), a manifestation of the lanthanide contraction.

In β-$ZrSb_2$, the Sb1−Sb2 distance (3.146(1) Å) falls in the Sb−Sb bonding range.[20] In LnAsTe, the As···Te distance ranges from 3.4425(8) Å in LaAsTe to 3.2820(4) Å in ErAsTe. Although we can find no structural data on other compounds that contain both As^{1-} and Te^{2-} ions, this distance appears to be short and suggestive of an interaction. For example, the As^{3+}−Te^{2-} distances in As_2Te_3 are 2.75 and 3.12 Å.[49] However, the band structure calculation described below does not support such an interaction.

The conductivity along the *b* axis (the direction of infinite zigzag As chains) as a function of temperature for PrAsTe, DyAsTe, and SmAsTe is shown in Figure 5. The compound PrAsTe exhibits good metallic behavior in this direction, whereas DyAsTe and SmAsTe have lower conductivities. The conductivities of PrAsTe, DyAsTe, and SmAsTe at room temperature are about 1.4×10^4, 5.7×10^2, and 4.2×10^1 S/cm, respectively, and that of β-$ZrSb_2$ is about 8.3×10^3 S/cm.[20] The metallic nature of PrAsTe was confirmed by the thermopower measurements, as shown in Figure 6, which indicate that PrAsTe is an n-type conductor.

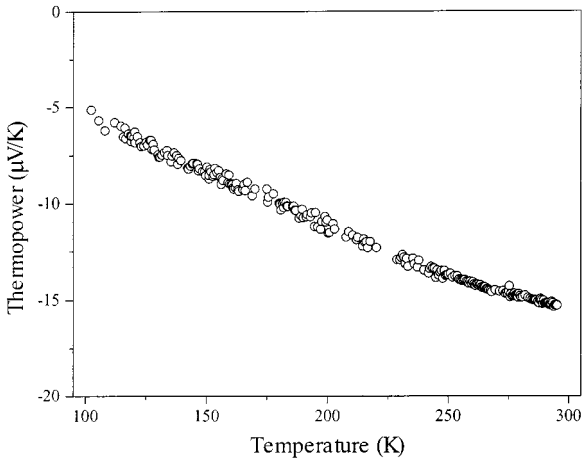

Figure 6. Thermopower vs temperature for PrAsTe.

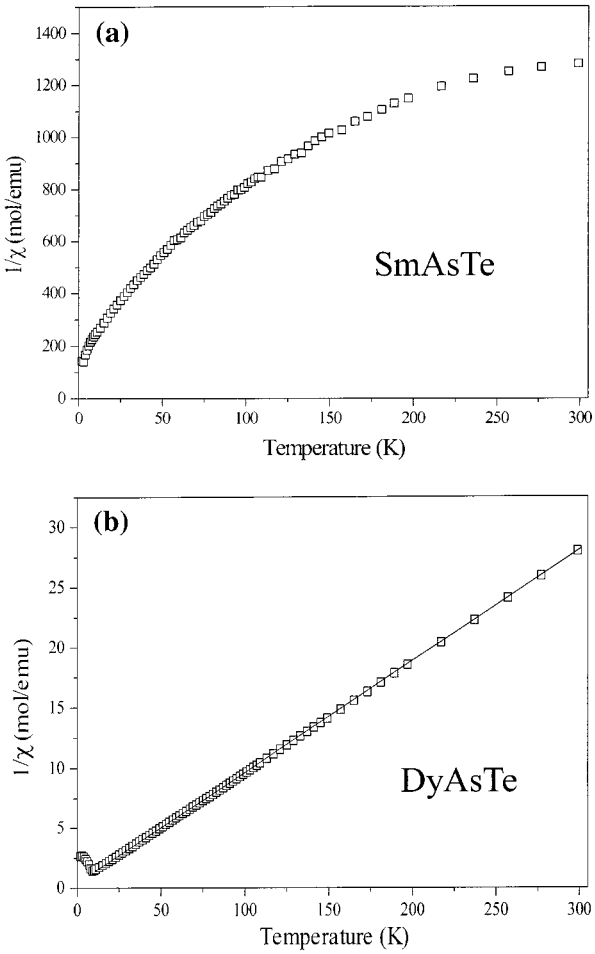

Figure 7. Plot of $1/\chi$ vs T for (a) SmAsTe and (b) DyAsTe.

Plots of $1/\chi$ versus T for SmAsTe and DyAsTe are shown in Figure 7. SmAsTe shows an antiferromagnetic transition at 3 K, and DyAsTe shows one at 9 K; transition temperatures are 2.0 K in $NdAs_{1-x}Se$ and 9.8 K in $DyAs_{1-x}Se$ ($x < 1$), which belong to the CeAsS family.[28] Above these transition temperatures SmAsTe and DyAsTe are paramagnetic. The magnetic susceptibility of SmAsTe does not follow a Curie−Weiss law because the effective magnetic moment of the 4f electrons has a temperature dependence arising from low-lying multiplets.[50]

(48) Schiferl, D.; Barrett, C. S. *J. Appl. Crystallogr.* **1969**, *2*, 30−36.
(49) Shu, H. W.; Jaulmes, S.; Flahaut, J. *J. Solid State Chem.* **1988**, *74*, 277−286.

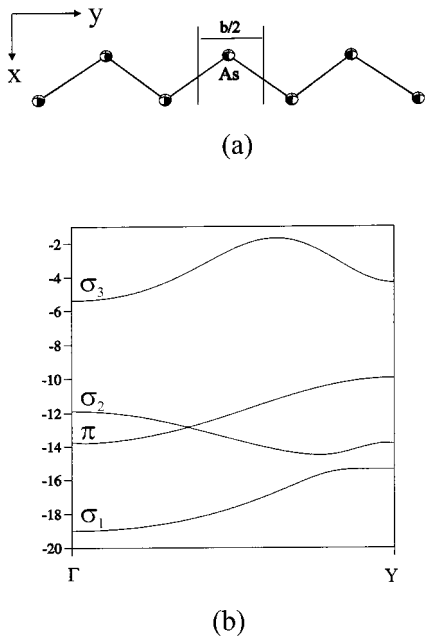

Figure 8. (a) Zigzag As chain in the local coordinate system. (b) Band structure of the zigzag chain based on the bond length and bond angle in LaAsTe, where Γ and Y are (0,0,0) and (0,1/2,0), respectively.

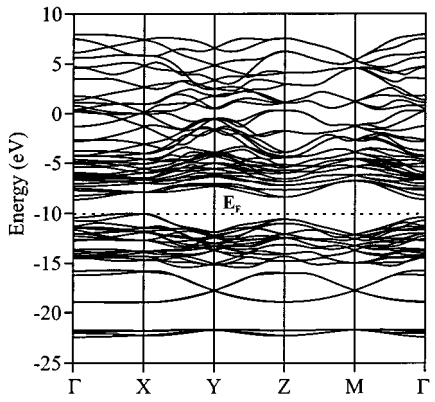

Figure 9. Band structure of LaAsTe, where Γ, X, Y, Z, and M are (0,0,0), (1/2,0,0), (0,1/2,0), (0,0,1/2), and (1/2,1/2,1/2), respectively.

The magnetic susceptibility of SmAsTe at room temperature is 1.4(2) μ_B, which is in good agreement with $\mu_{eff} = 1.66\ \mu_B$ calculated from Van Vleck's formula for Sm^{3+} with a screening constant $\sigma = 34$ for 300 K.[50] DyAsTe follows the Curie−Weiss law $\chi = C/(T - \theta)$, with $C = 13.33(11)$ emu/mol and $\theta = -7.53(15)$ K. The calculated effective magnetic moment of 10.33(5) μ_B for DyAsTe agrees with the theoretical value of 10.65 μ_B for Dy^{3+}.[51]

Given that there are no Te···Te interactions in these structures (the shortest Te−Te distances are 4.0084(9) Å in LaAsTe and 3.7361(4) Å in ErAsTe), that the As−As bond lengths correspond to single-bond distances, and that the effective magnetic moments are consistent with Ln^{3+}, formal oxidation states of 3+, 1−, and 2−, respectively, may be assigned to Ln, As, and Te in LnAsTe. Thus, each As atom carries one negative charge, makes two single bonds with two neighboring As atoms in the chain, and has a stable electronic configuration. To confirm this, an extended Hückel tight binding calculation was made on an infinite undistorted zigzag As chain (Figure 8a) in LaAsTe. The band structure is displayed in Figure 8b. The σ_1 band (mainly 4s orbitals) is at low energy, the bonding σ_2 band (mainly $4p_x$ and $4p_y$) and the π band ($4p_z$) are at about the same intermediate energy, and the antibonding σ_3 band (mainly $4p_x$ and $4p_y$) is at high energy. If we fill all the bands except the antibonding σ_3 band, six electrons are needed and the As atom carries a charge of −1, as deduced above from geometrical considerations. The entire band structure of LaAsTe is shown in Figure 9. The band gap does not vanish with the introduction of La and Te. The overlap between As and Te is −0.03 (!), as opposed to that of about 0.16 between atoms Sb1 and Sb2 in β-$ZrSb_2$.[20] Nor is an As···Te interaction indicated in a TB-LMTO calculation. Nevertheless, if there were some interaction, then the metallic nature of these compounds could be rationalized, but not the striking differences so evident in Figure 5.

Acknowledgment. This research was supported by NSF Grant DMR97-09351. Use was made of the Central Facilities supported by the MRSEC program of the National Science Foundation (DMR96-32472) at the Materials Research Center of Northwestern University. P.B. was supported by NSF Grant DMR96-32472.

Supporting Information Available: X-ray crystallographic files in CIF format for the structure determinations of LaAsTe, PrAsTe, SmAsTe, GdAste, DyAsTe, and ErAsTe. This material is available free of charge via the Internet at http://pubs.acs.org.

IC000187V

(50) Van Vleck, J. H. *The Theory of Electric and Magnetic Susceptibilities*; Oxford University Press: London, 1932.
(51) Hatfield, W. E. In *Solid State Chemistry: Techniques*; Cheetham, A. K., Day, P., Eds.; Clarendon Press: New York, 1987; pp 122−162.
(52) Shannon, R. D. *Acta Crystallogr., Sect. A: Cryst. Phys., Diffr., Theor. Gen. Crystallogr.* **1976**, *32*, 751−767.